Doerr, Martin and Apostolis Sarris (eds) 2003. The Digital Heritage of Archaeology. CAA2002. Computer Applications and Quantitative Methods in Archaeology. Proceedings of the 30th CAA Conference, Heraklion, Crete, April 2002.

Profile Segmentation Scheme for Automated Classification of Archaeological Sherds

Martin Kampel, Robert Sablatnig and Hubert Mara

Vienna University of Technology, Institute of Computer Aided Automation,
Pattern Recognition and Image Processing Group
Favoritenstr. 9/183-2, A-1040 Vienna, Austria
{kampel,sab,mara}@prip.tuwien.ac.at

Abstract. Motivated by the requirements of present day archaeology, we are developing an automated documentation system for archaeological classification and reconstruction of ceramics. Our system works with the profile of an archaeological fragment, which is the cross-section of the fragment in the direction of the rotational axis of symmetry. Ceramic fragments are recorded automatically by a 3D-measurement system based on structured (coded) light. The input data for the estimation of the profile is a set of points produced by the acquisition system. A function fitting this set should be constructed and later on processed to find the extremal and inflection points necessary to classify the original fragment. The one we propose is based on cubic B-splines. This paper shows a method for shape classification of archaeological fragments.
Keywords. classification, segmentation, pottery, splines

1 Introduction

Motivated by the requirements of present day archaeology, we are developing an automated system for archaeological classification of ceramics. Ceramics are among of the most widespread archaeological finds, having a short period of use. Since the 19th century, the physical characteristics of archaeological pottery have been used to assess cultural groups, population movements, inter-regional contacts, production contexts, and technical or functional constraints (archaeometry). Because archaeometry of pottery still suffers from a lack of methodology, it is important to develop analytical classification tools of artefacts (Orton C., Tyers P., and Vince A., 1993). A large number of ceramic fragments, called sherds, are found at every excavation. These fragments are documented through photographs, measurements and drawings; then they are classified. The purpose of *classification* is to get a systematic view on the excavation finds.

Traditional archaeological classification is based on the so-called profile of the object, which is the cross section of the fragment in the direction of the rotational axis of symmetry. This two-dimensional plot holds all the information needed to perform archaeological research. The correct profile and the correct axis of rotation are thus essential to reconstruct and classify archaeological ceramics.

Fragments of vessels are thin objects, therefore 3D-data of the edges of fragments are not accurate and this data cannot be acquired without placing and fixing the fragment manually. Ideally, the fragment is placed in the measurement area, a range image is computed, the fragment is turned and again a range image is computed. To perform the registration of the two surfaces, we use a-priori information about fragments belonging to a complete vessel: both surfaces have the same axis of rotation since they belong to the same object. Using the axis of rotation based registration technique, (Sablatnig R. and Kampel M., 2002) a profile is generated automatically. Furthermore the rotational axis is used for the proper orientation of the fragments.

For classification into the different types of vessel the profile is used. Archaeologists use the number of extremal points and their distance ratios to determine which type of vessel a sherd belongs to. (Ettlinger, et. Al, 1990)

The next section explains the acquisition and processing of the 3D-data in order to archive the profile section. Section 3 describes the automatically segmentation of the profile for the correct classification of the fragment. Results are presented in Section 4. The paper concludes with a discussion of the results and gives an outlook on future research.

2 Data Acquisition & Processing

In our system, the profile sections are achieved automatically by a 3D-measurement system based on structured (coded) light technique. Shape from structured light is a method, which constructs a surface model of an object based on projecting well-defined light patterns onto the object. The image, together with the knowledge about the pattern and its relative position to the camera are used to calculate the coordinates of points belonging to the surface of the object (Kampel M. and Sablatnig R., 1999).

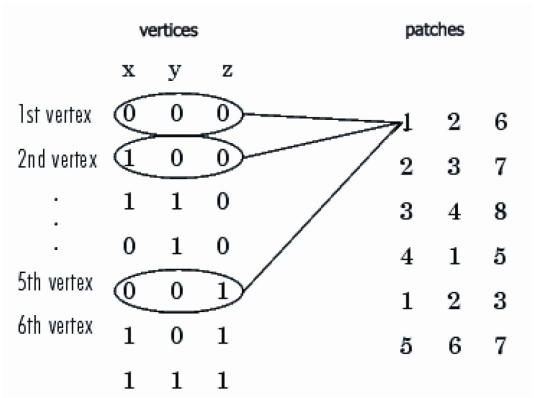

Fig. 1. *Connected vertices along patch edges.*

The 3D-data is stored as 3D-points (called vertices) that are connected in form of triangles (called patches). These vertices and patches are stored in an indexed list. A sample of vertices and patches is shown in Fig.1.

Every patch consists of three indices to the corresponding vertices and for every patch the texture is stored as RGB-value. This kind of representation has been selected to export and import the data as VRML-file in order to enable software independency.

We use the oriented sherd for the estimation of the longest profile line, which is supposed to be the longest elongation along the surface of the sherd parallel to the rotational axis *rot* through two points $\{p_{r1}, p_{r2}\}$. This profile line is located where the fragment has its maximum height h_{max}. The height h_i is defined as the orthogonal distance from a point p_i of the sherd to the orifice plane of the object. For every point of the 3D-model of the sherd the height has to be calculated and point p_{max} with maximum height $h_{max} = max(h_i)$ is selected. Next, the parameters for the intersecting plane $e = \{p_{r1},p_{r2},p_{max}\}$ spanned through the points of the rotational axis *rot* and this point p_{max} are calculated.

With the parameters of plane e that intersects the fragment where the longest profile line is located the distances between the plane e and each vertex of the 3D-model are calculated. Then the nearest 1% of points are selected as candidates for the profile. For each of those vertices all patches they belong to are filtered by a search in the patch list with their index number. In Fig 2 a sherd shaded by the value of distance is shown (lighter means nearer to the intersecting plane).

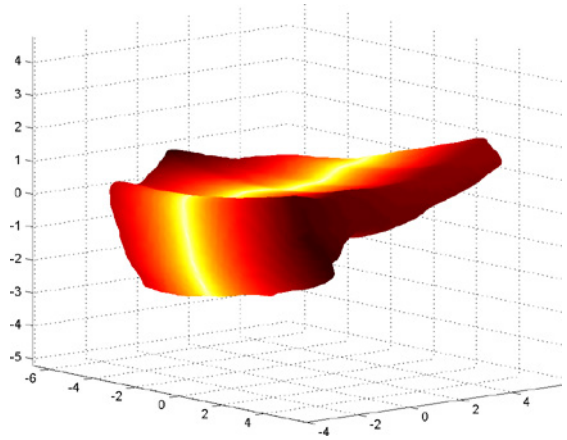

Fig. 2. *Nearest points of the sherd to the plane.*

As mentioned before every patch is a triangle, which consists of three points that are connected through three lines. For all three combinations of pairs of points of the filtered patches the position is calculated using the Hessian normal form $ax^2 + by^2 + cz^2 = 0$. The result of the Hessian normal form is the distance to the plane and the sign corresponds to the side - left or right – where the point is located. Every pair of vertices that has both points on different sides of the plane is part of the profile line, because its connection intersects the plane. The coordinates of these pairs are rotated into the xy-plane and the z-coordinate is removed. The result is a proper oriented profile line (Fig. 3).

This profile line is stored as indexed list *pli* of 2D-coordinates $p_i = (p_{i1},p_{i2})$ of curvature points and a list of index pairs $con = (\{i,,j\})$. These index pairs represent the connection between the points p_i. The pairs of vertices of the profile line are sorted, so that each point p_i in the list is connected to its immediate neighbour p_{i-1} and p_{i+1}. The profile is stored as a single closed list of connected pairs of points. The indexed list *pli* and the list of pairs *con* are transformed into an indexed list *rel* of angles α_i and distances d_i between connected pairs of points and the coordinate of the first point $p_{i=1}$ of the indexed list *pli*. This representation is used for segmentation of the profile-line, explained in the next section.

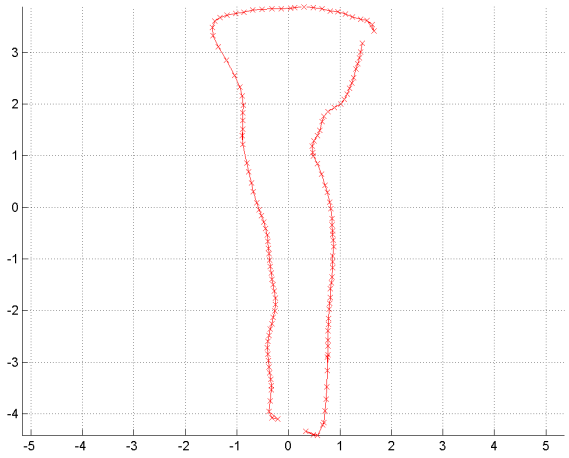

Fig. 3. *Estimated oriented profile.*

3 Segmentation of the profile section

Following the manual strategy of the archaeologists, the profile should first be segmented into its parts, the so-called *primitives*, in an automatic way. The profile determined has to be converted into a parameterized curve (Shoukry A. and Amin A., 1983, Hu Z. and Ma S.D., 1995) and the curvature has to be computed (Bennett J.R. and MacDonald J.S. 1975, Matas J., Shao Z., and Kittler J.V. 1995). Local changes in curvature (Rosenfeld A. and Nakamura A, 1997) are the basis for rules required for segmenting the profile. Our approach is a hierarchical segmentation of the profile into rim, wall, and base by creating segmentation rules based on expert knowledge of the archaeologists and the curvature of the profile. The segments of the curve are divided by so called segmentation points. If there is a corner point, that is a point where the curvature changes significantly, the segmentation point is obvious. If there is no corner point, the segmentation point has to be determined mathematically.

Several points characterize the curve. Fig. 4 shows the segmentation scheme of an S-shaped vessel as an example. A set of points is defined like,

- Inflexion point (IP): point, where the curvature changes its sign;
- Local maximum (MA): point of vertical tangency;
- Local minimum (MI): point of vertical tangency;

- Orifice point (OP): outermost point, where the profile line touches the orifice plane;
- Base point (BP): outermost point, where the profile line touches the base plane
- Point of the axis of rotation (RP): point, where the profile line touches the axis of rotation.

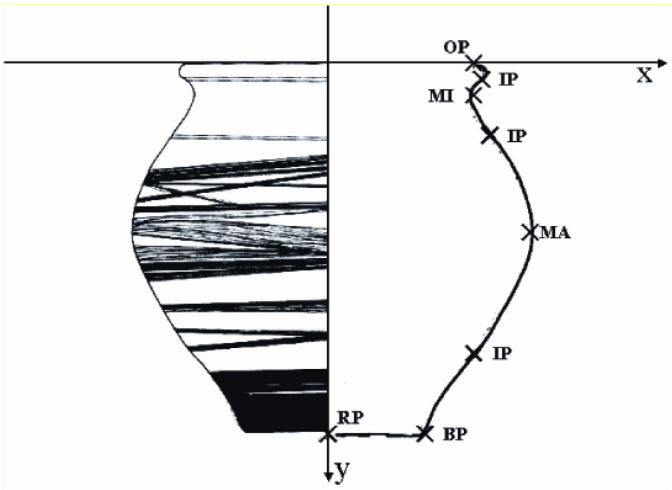

Fig. 4. *S-shaped vessel: profile segmentation scheme.*

By means of these curve points several main segments of a vessel are distinguished: rim, upper part, lower part, neck, shoulder, belly and bottom. On the basis of the number and characteristics of these segments different kinds of vessels can be classified. Segmentation is done only on the outer half of the profile (Orton C., Tyers P., and Vince A., 1993), because the inner side does not contain information. So the profile is divided in the outer and inner profile at the orifice and the bottom point, which is calculated by knowledge of the orientation. The next step is to split the outer profile into its primitives by locating the characteristic points. These points are found within the transformed data from Section 2: For each point p_j the change of angle is calculated as angle between the vector $p_i - p_j$ and the vector $p_j - p_k$ shown in Fig. 5.

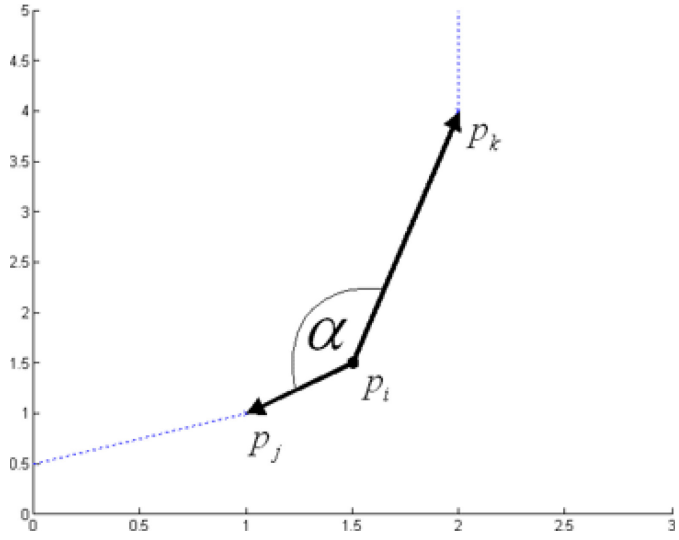

Fig 5 part of the profile line

This is done using angles in the transformed data rel. The list of changing angles are smoothed with multi-spline-representation (Adler K., et al 2001), so that distortions are eliminated and the characteristic points for further classification in the curvature can be calculated.

Our formalized approach uses mathematical curves to describe the shapes of the vessels and their parts. The profile is thus converted into one or more mathematical curves. We apply four methods for interpolation and four methods for approximation by B-splines on the reconstruction of the vessel profiles (i.e. the profiles are projected into the plane).

3.1 Interpolation by Cubic Splines

The following definitions were adopted from (DeVore and Lorentz G., 1993). We suppose that the planar closed curve r to be fitted (interpolated or approximated) will be represented by parametric equations

$$r(t) = [x(t), y(t)] \quad \textbf{(1)}$$

in an interval in the Cartesian coordinates of R^2. The curve has continuous second derivatives. The curve is given by a set of points $P_i = [x(t), y(t)]$ together with the non-decreasing sequence of knots $\{t_i, i = 1,...,n+1\}$ of parameter t. Constructing a curve $S(t)$, which approximates the function given by the points can be done by a cubic spline with an adequate parameterization and external conditions. The curve must be initially divided into sub-intervals, where functional approximation and interpolation methods can be applied.

The support of a cubic spline is 5 intervals. Denote by B_i^4 an $k-th$ order spline $(k \le 3)$ whose support is $[t_i, t_{i+4}]$. Then, it is possible to normalize these splines so that for any $x \in [a,b]$

$$\sum_{i=-3}^{n+3} B_i^4(x) = 1 \quad \textbf{(2)}$$

Any cubic spline $S_n(x)$ with knots $t_{0,...,tn}$, and coefficients $a_{-3}, a_{-2},..., a_n$, can be written in the form

$$S_n(x) \sum_{i=-3}^{n} a_i B_i^4(x) \quad \textbf{(3)}$$

There are $n+3$ coefficients a_i in equation 3 showing that the vector space of cubic splines has dimension $n+3$, so that the $n+1$ functional values will not determine $S_n(x)$ uniquely – two additional constraints must be supplied. Cardinality of the basis has been sacrificed for small support in the basis. Consequently, in evaluating $S(x)$ for any $x \in [a,b]$, only four terms at most in the sum (3) will be non-zero.

The basis cubic splines can be constructed by the following recurrent relationship:

$$B_i^n(x) = \frac{x - t_i}{t_{i+n-1}} B_i^{n-1}(x) + \frac{t_{i+n} - x}{t_{i+n} - t_{i+1}} B_{i+1}^{n-1}(x), \quad \textbf{(4)}$$

$i = -3,...n-1$ and $n = 1,2,3,4$. A useful convention is to define the first-order splines as *right-continuous* so that

$$B_i^1(x) = \delta_i \ for \ x \in [t_i, t_{i+1}], i = -3,-2,...,n+3 \quad \textbf{(5)}$$

The method is of local character: the change of the position of one control vertex influences only 4 segments of the curve. The resulting curve is in particular coordinates a polynomial of 3rd degree for $t \in (t_j, t_{j+1})$ and has continuous all derivatives in these coordinates.

Since $B_i^n(x)$ is nonzero only on the interval $[t_i, t_{i+4}]$, the linear system for the B-spline coefficients of the spline to be determined, by interpolation or least-squares approximation, is banded, which makes the solving of that linear system particularly easy.

$$S^4(x_j) = \sum_{i=0}^{n} B_i^4(x_j) a_i = y_j, \quad j = 0,...,n \tag{6}$$

We selected four interpolation methods:

a) Cubic spline interpolation with Lagrange end-conditions $cs1$ (i.e. it matches end slopes to the slope of the cubic that matches the first four data at the respective end);
b) Cubic spline interpolation with not-a-knot end-condition $cs2$
c) Spline interpolation with an acceptable knot sequence $cs3$;
d) Spline interpolation with an optimal knot distribution $cs4$. As 'optimal' knot sequence the optimal recovery theory of Micchelli, Rivlin and Winograd (Micchelli T. and Winograd S., 1976) is used for interpolation at data points $\tau(1),...,\tau(n)$ by splines of order k;

All the discussed interpolation methods satisfy the Schoenberg-Whithey conditions, i.e. the achieved representation is for the method, the given data and knot sequences unique. These methods were applied to each of the intervals of the curve, and compared from the point of view of their approximation error (least mean square of the differences of the input value and the spline value) on the given data.

We made a surprising observation: Spline interpolation with an acceptable knot sequence in all intervals of all profiles approximated the data with a smaller error than spline interpolation with optimal knot distribution.

We select an 'optimal' method according to the following criteria: The first criterion for selection of the most appropriate interpolation method is the minimal approximation error on the data in the corresponding interval. To rule out ambiguity, the second criterion is applied: minimal length of the knot sequence corresponding to the method. For further exclusion of ambiguity, the third criterion is applied: The priority of the interpolation method is based on the statistical observations. The priority of the methods was achieved experimentally on profiles and their particular intervals and expresses a 'statistical' ordering according to the smallest approximation error over all intervals of the tested profiles.

3.2 Approximation by Cubic B-Splines

Since in the task being solved, the amount of data pairs acquired to describe a vessel or its parts do not always suffice to represent the shape of the vessel reliably, interpolation does not have to be always the appropriate method. From this reason, we compared the approximation methods on representing the overall shape of the whole curve with respect to the interpolation methods.

The following approximation methods were applied and compared:

a) Cubic smoothing spline with the smoothing parameter $p > 0\ (cs5)$;
b) Smoothing spline with the smoothing parameter; $tol > 0\ (cs6)$
c) Least squares spline approximation with the number of knots equal to a half of the amount of the data $(cs7)$;
d) Least squares approximation with the number of knots equal to the number of data - degree of the spline in the particular interval $(cs8)$;

4 Results

When the most appropriate interpolation and approximation methods are computed and selected for each of the intervals of the curve, the method with a smaller error (in case of ambiguity, the interpolation method is preferred) is selected for the interval. The approximation error of the representation over the whole curve is computed. This representation is unique and optimal with respect to the above-mentioned criteria. The method was tested on computed profiles like shown in Fig. 6.

Fig. 6. *Profiles of different fragments.*

All interpolation and approximation methods are applied for every sub-interval of the curve after each run of the program. While the curve is generated gradually for each sub-interval of the curve, the overall approximation error is computed. As a result the profile is constructed from the selected methods and is compared to the data set.

Table 1 displays the approximation errors for all methods in all intervals of the leftmost profile in Fig 6, including the selected interpolation and approximation methods for the corresponding interval and the selected overall method for the whole profile. The whole data sets contained approximately 350 data points and the length of the whole curve was approximately 400 points.

method / interv.	1	2	3	4
cs1	0,2163	0	0.6047	0.0781
cs2	0,2163	0	0,5994	0,0782
cs3	0,2163	0	0,5994	0,0782
cs4	0,2163	0,6169	2,1080	0,0877
cs5 (tol = 5)	0,2163	2,3114	0,5994	1,1816
cs6 (p = 1)	0,1350	0	0,6229	0,0781
cs7	0,2163	5,9470	5,5298	0,5015
cs8	0,2163	0,0032	0,6014	0,1308
select. intp.	1	1	2	1
select. appr.	6	6	5	6
overall	6	1	2	1

method / interv.	5	6	7	8
cs1	1,1685	2,2497	1,1424	0,0884
cs2	1,1686	2,2514	0,1433	0,0884
cs3	1,1686	2,2514	0,1430	0,0883
cs4	1,4510	2,3485	0,1615	0,0991
cs5 (tol = 5)	2,9430	2,2514	2,2073	0,0884
cs6 (p = 1)	1,1687	2,2496	0,1646	0,0884
cs7	6,9127	6,2323	0,8617	1,0675
cs8	1,1850	3,8347	0,1430	0,2551
select. intp.	1	1	1	1
select. appr.	6	6	8	6
overall	1	6	1	6

Table 1. *Approximation errors for all methods in 8 intervals.*

The most frequently selected interpolation method was cs1 and the most frequently selected approximation method was cs6 in our experiments. An interpolation method was preferred in the intervals, where a sufficient number of data with respect to the length of the interval was given. An approximation method was preferred in the intervals, where there was a lack of data.

Fig. 7 right half shows one example of an automatically segmented pot with the characteristic points detected and the appropriate manual segmentation on the left of Fig. 7. Another example of automatic segmentation is shown on Fig.8. Processing time for all fragments tested was less then 10 seconds.

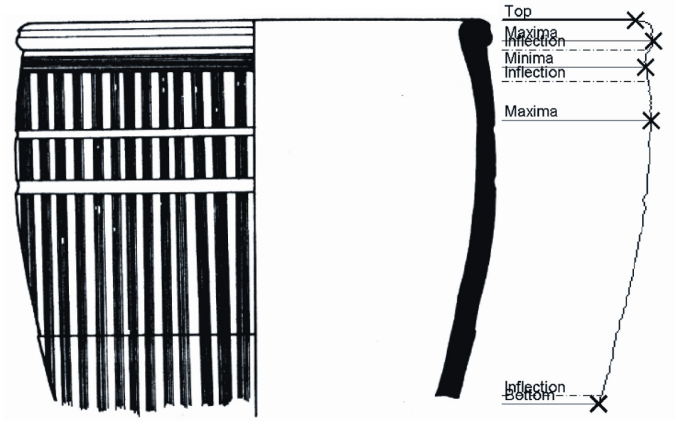

Fig. 7. *Manual drawing and detected classified.*

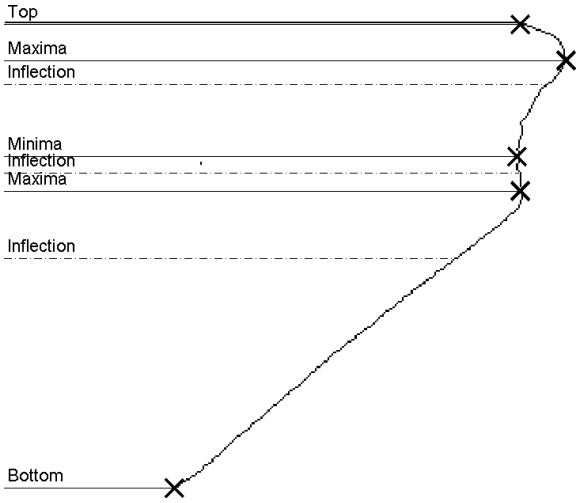

Fig. 8. *Detected characteristic points.*

Conclusion and Outlook

The method presented for selection of an 'optimal' representation (optimal with respect to the considered methods and selection criteria) of a 2D profile of an archaeological fragment computes and displays a unique solution. The achieved fragment representations, the first part of an automated system for classification of archaeological fragments, are the input of the second part, the classification.

The profile parts, the so-called profile primitives, are used to perform the classification. The segmentation (division) into primitives depends on the orientation of the fragment. In order to achieve a unique representation, it is important to set a unique orientation for all fragments. The classification will be solved in the high dimensional real space and therefore the uniqueness and the high precision of the profile representation are very important.

The method has been tested on synthetic and real data with reasonable good results, the accuracy of the method is sufficient since the computed position of the characteristic points is much more precise and more objective than the manually estimated positions performed by archaeologists. The current task is to do extensive experiments in order to meet all archaeological requirements and to show the applicability of the approach.

Acknowledgments

The authors would like to thank Prof. Marc Waelkens and Roland Degeest from the Katholieke Universiteit Leuven, Eastern Mediterranean Archaeology and Kristina Adler and Martin Penz from Vienna University, Institute of Classical Archaeology for their archaeological support and contributions in evaluating the profile representation approach and for helpful and inspiring discussions.

References

ADLER, et.al. Computer aided classification of ceramics achievements and problems. In *Proc. of 6th Intl. Workshop on Archaeology and Computers*, Nov 2001.

BENNETT J.R. and MacDONALD J.S.. On the Measurement of Curvature in a Quantized Environment. *IEEE Trans. Computer*, 24:803–820, 1975.

DEVORE R. and LORENTZ G. *Constructive Approximation*, Springer, 1993.

ETTLINGER, et. al. *Conspectus Formarum Terrae Sigillatae Italico Modo Confectae*. Dr. Rudolf Habelt GMBH, Bonn, 1990.

HU Z. and MA S.D. The Three Conditions of a Good Line Parameterization. *Pattern Recognition Letters*, 16:385–388, 1995.

KAMPEL M. and SABLATNIG R.. On 3d Modelling of Archaeological Sherds. In *Proceedings of International Workshop on Synthetic-Natural Hybrid Coding and Three Dimensional Imaging, Santorini, Greece*, pages 95–98, 1999.

MATAS J., SHAO Z., and KITTLER J.V. Estimation of Curvature and Tangent Direction by Median Filtered Differencing. *8th International Conference on Image Analysis and Processing*. Pages 83–88, 1995.

ORTON C., TYERS P., and VINCE A.. *Pottery in Archaeology*, 1993.

ROSENFELD A. and NAKAMURA A.. Local Deformations of Digital Curves. *Pattern Recognition Letters*, 18(7):613–620, July 1997.

SABLATNIG R. and KAMPEL M. Model-based registration of front- and backviews. *Computer Vision and Image Understanding*, page to appear, 2002.

SHOUKRY A. and A. AMIN. Topological and Statistical Analysis of Line Drawings. *Pattern Recognition Letters*, 1:365–374, 1983.

MICCHELLI T. R. C. A. and WINOGRAD S. The Optimal Recovery of Smooth. *Functions*. *Numerische Mathematik*, 26:191 200, 1976.